Modelling of flow through the circle of Willis and cerebral vasculature

I. D. Šutalo[1,2], A. Bui[1], S. Ahmed[1], K. Liffman[1,2] & R. Manasseh[1]
[1]*Materials Science and Engineering, Commonwealth Scientific and Industrial Research Organisation (CSIRO), Australia*
[2]*School of Public Health, Curtin University of Technology, Australia*

Abstract

The blood flow through the circle of Willis was modelled by coupling a Computational Fluid Dynamics (CFD) model of the circle of Willis with a branching tree model of the cerebral vasculature. The cerebral small vascular networks, which often cannot be accurately obtained by medical imaging, were modelled using a branching tree fractal model that accurately simulated the cerebral vasculature geometries and flow. This provided realistic mass flow boundary conditions for the outlet arteries of the circle of Willis.

CFD was used to model the three-dimensional transient flow through a simplified and a patient-specific circle of Willis. The patient specific geometry was obtained directly from Computed Tomography (CT) images. A pipe network model was also used to predict the flow through the simplified circle of Willis and the predictions for the flow rates were within 4% of the CFD predictions. The coupled CFD and branching tree model provided useful insight into the variation of the flow through the circle of Willis.

Keywords: circle of Willis, cerebral hemodynamics, computational fluid dynamics, cerebral circulation, carotid arteries, numerical models.

1 Introduction

Blood flows into the circle of Willis (CoW) system via the vertebral (VA) and internal carotid arteries (ICA) and flows out via the posterior (PCA), middle (MCA) and anterior (ACA) cerebral arteries. At the CoW periphery the out-flowing blood enters a network of cerebral arterioles and capillaries. The resistance within the brain cerebral small vasculature is non-homogeneous and may change the flows through the ICA and VA.

WIT Transactions on Biomedicine and Health, Vol 13, © 2009 WIT Press
www.witpress.com, ISSN 1743-3525 (on-line)
doi:10.2495/BIO090081

Most previous numerical studies on the CoW have investigated occlusions in the ICA or VA, or anatomical variations within the CoW. There have been several simplified and one-dimensional (1D) models of the blood flow through the CoW. Kufahl and Clark [1] developed a 1D finite difference model with elastic walls. Hillen *et al* [2] developed a 1D non-linear model. The peripheral resistances were determined from mass fluxes and anatomical structure. Linear models were also developed [3–5]. Other simplified and 1D models were compared to experimental data or observations [6–13]. Of these models, the Alastruey *et al* [10] model with compliant vessels compared anatomical variations and occlusions for common CoW geometries.

Computational Fluid Dynamics (CFD) models of the CoW include a 2D non-linear model with time varying resistances [14, 15]. There have been several CFD studies on 3D patient-specific models of the CoW that considered anatomical variations. Cebral *et al* [16] modelled the flow through 3D patient-specific models of the CoW. They compared flow resistances calculated from flow simulations with those obtained using a vascular bed model based on parallel resistors. Moore *et al* [17, 18] modelled three anatomical variations and showed the flow redistribution with these anatomical variations. Kim *et al* [19, 20] modelled three patient-specific geometries and found communicating arteries play an important role in the cerebral autoregulation mechanism. Alnaes *et al* [21] modelled three geometric variants of the posterior part of the CoW and showed that differences in vessel radii and bifurcation angle influence the wall shear stress. Most of these CFD models included autoregulation [14, 15, 17–20] and only Kim *et al* [19] and Kim [20] modelled flexible walls.

In the CFD simulations of the CoW the vascular bed resistance models used for the outlet boundary conditions include: network of resistors [16, 19, 20], porous media as terminating blocks [14, 15, 17, 18], constant pressure [21] and calculating flow resistance of branching tree models [16]. Cebral *et al* [16] recommended using arterial models to specify outflow conditions and include arterial compliance.

To describe the outflow boundary conditions in the CFD CoW modelling, previous work usually used network resistances or porous media models for the peripheral resistances rather than calculating them from a branching tree model of the cerebral vasculature. This study investigates the effect of changes in peripheral resistances of the CoW on the flow through the ICA and VA without occlusions. A coupled CFD and branching tree model was developed where a 3D CFD model of the CoW was coupled with a branching tree fractal model of the cerebral vasculature.

2 Methods

2.1 Branching tree model for cerebral vasculature

Fractal branching tree models were created for all territories of cerebral vasculature, namely ACA, MCA, and PCA, using the Constrained Constructive Optimisation (CCO) method [22]. The fractal scaling parameter of the branching

tree models was chosen so that the generated fractal models are physiologically correct for the description of the human cerebral vasculature. With the systemic and venous pressures prescribed, the transient flow rates at the six outlets of the CoW were obtained using the pulsatile flow model developed for a fractal vascular network, which is described in more detail in a previous work [22]. Coupling of the CFD and fractal tree models was carried out by applying these flow rates as boundary conditions in the CFD simulations. The branching tree predicted peripheral resistance ratios for the ACA, MCA, and PCA for a normal person were: 6.906, 3.453, and 4.615, respectively. This fractal tree model more accurately simulates the cerebral vasculature geometry and peripheral resistances of the CoW than previous models, and includes wall compliance and viscosity change due to artery size [22].

2.2 Pipe network model

A commercial pipe network code Design Flow Solutions (ABZ Incorporated, Chantilly, Virginia USA) was used to investigate the steady-state flow through the CoW. The dimensions for the simplified complete CoW were taken from Hillen *et al* [2]. The network of arterioles and capillaries produces a pressure drop in the cerebral arterial system from an average inlet pressure of around 100 mmHg to pressures approaching venous pressures of around 10 mmHg [2]. The outlet boundary conditions at the periphery of the CoW for the CFD model were obtained from the branching tree model.

2.3 Computational fluid dynamics model

The CFD model simulated the 3D transient incompressible laminar pulsatile flow fields through the CoW. The numerical modelling was performed using the commercial CFD package ANSYS CFX-11, which has a coupled solver and uses an unstructured mesh based on the finite element method. The inlet boundary condition was set by specifying a pressure pulse ranging 80–125 mmHg at the inlet for a period of 0.7 s. The outlet boundary conditions were pulsatile flow rate obtained from branching tree model. The density of the blood was assumed to be 1050 kg/m^3, and the blood flow was assumed to be Newtonian. The mesh consisted of tetrahedral elements, and the solutions were mesh-independent when the total number of elements was 267,440 for the simplified geometry and 74,250 for the patient-specific geometry. The dimensions of simplified CoW geometry were the same as used in the pipe network model. The average Reynolds number based on the ICA diameter for the simplified and patient-specific CoW geometries were about 400.

The patient-specific geometry data was acquired from CT scans and converted to surface (STL) and then finite element models using Slicer-3D, meshlab and ICEMCFD. The patient-specific geometry was more complex than the symmetrical simplified CoW geometry. This patient-specific geometry was missing the left posterior communicating artery (PCoA) and had a penal anterior communicating artery 1 (ACA1). This anatomical configuration with missing PCoA occurs in 9% of the population [10].

3 Results and discussion

3.1 CFD predictions of carotid and vertebral artery flow rates for the simplified CoW geometry

Modelling runs with the coupled CFD and vascular tree fractal model investigated the effect on the VA and ICA flow rates of reducing by 10% the diameters of the peripheral vasculature of the ACA, MCA and PCA, respectively.

For a normal person with a complete CoW, under the peripheral resistance conditions stated earlier, the CFD model predicted that 69% of the blood flow enters the simplified CoW geometry via the ICA and 31% enters via the VA. When the diameters of the ACA peripheral vasculature was reduced by 10% then 66% of the blood flow entered the CoW from the ICA, and 34% entered via the VA. A 10% decrease in the diameters of the MCA peripheral vasculature reduced the flow through the ICA further so that 64% of the blood flow entered the CoW from the ICA and 36% entered from the VA. However, a 10% decrease in the diameters of the PCA peripheral vasculature decreased the flow through the VA so that 76% of the flow entering the CoW entered via the ICA, and 25% entered via the VA. A summary of results showing the ICA and VA flow rates for the different peripheral resistances are given in table 1.

Table 1: Percentage blood flow rates through the ICA and VA as obtained from the CFD simulations for the simplified and patient-specific CoW geometries compared to the pipe-flow code simulations.

Resistance Ratio (ACA: MCA: PCA)	% ICA			%VA		
	pipe simple	CFD simple	CFD patient specific	pipe simple	CFD simple	CFD patient specific
normal 6.906:3.453:4.615	70	68.6	74.4	30	31.4	25.5
increased ACA resistance 10.526:3.453:4.615	68	66.3	72.3	32	33.7	27.7
increased MCA resistance 6.906:5.263:4.615	66	63.7	69.7	34	36.3	30.3
increased PCA resistance 6.906:3.453:7.034	77	75.5	81.0	23	24.5	19.0

Fig. 1 shows the pressure distribution at peak systole in the simplified CoW geometry where the pressure is highest at the VA and ICA inlets and then decreases along the CoW. Fig. 2 shows that there is negligible change in VA flow rate magnitude for a 10% decrease in diameters of the peripheral vasculature of the ACA and MCA, most of the decrease occurs in the ICA flow rate. While for a 10% decrease in the diameters of the PCA vasculature most of the flow rate decrease occurs in the VA.

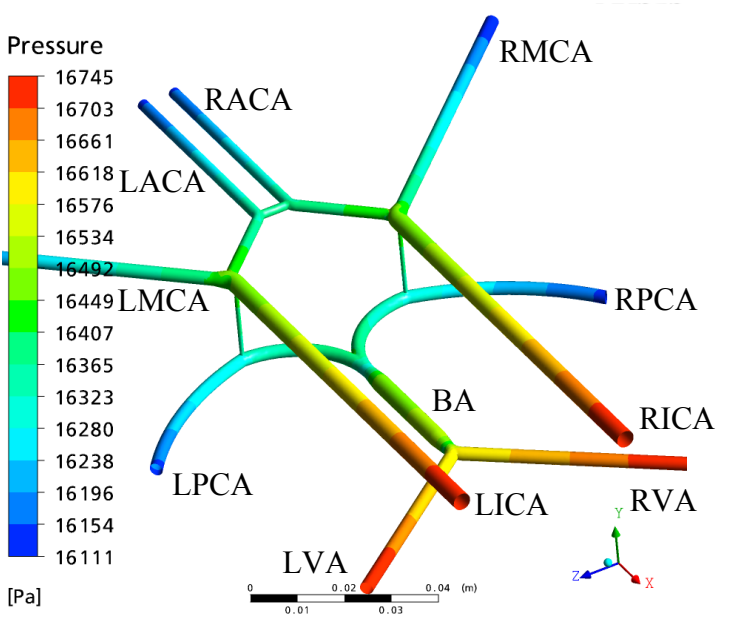

Figure 1: Instantaneous pressure on walls of simplified CoW at peak systole. The two VA merge into the basilar artery (BA).

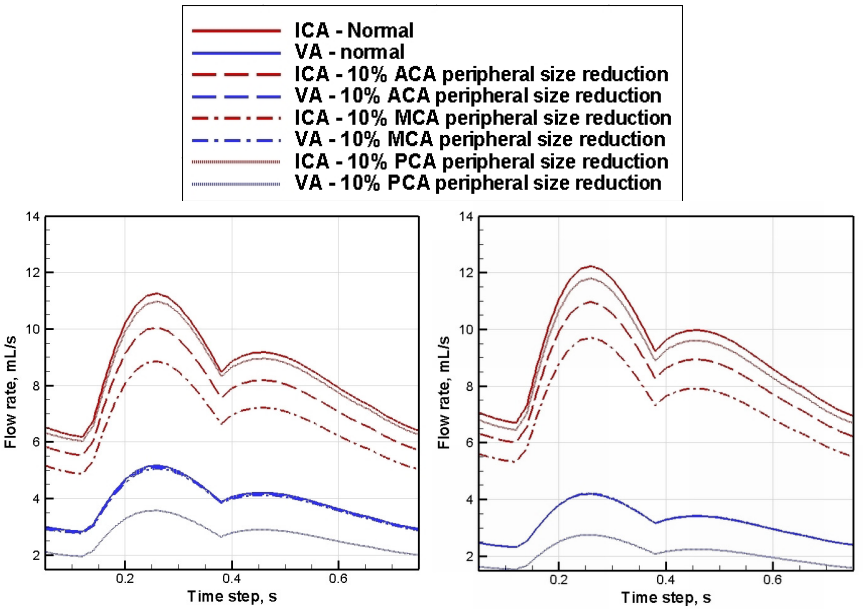

Figure 2: CFD predictions of inlet flow rates in the simplified (left) and patient-specific (right) CoW.

3.2 Comparisons between CFD and pipe network model predictions

The pipe network model predictions for the inlet flow rates to the CoW were within 4% of the CFD predictions with the simplified CoW geometry as shown in table 1. A major difference between the two models was the run time: 3 hours for the CFD code compared to a few seconds for the pipe flow model. However, the pipe network model results were for steady-state flow, while the CFD results were for pulsatile flow and showed the whole pulsatile flow rate profile.

3.3 Patient-specific CoW geometry model predictions of carotid and vertebral artery flow rates

The patient-specific CoW geometry simulations show significant changes of the VA and ICA flow rates when compared to the symmetric simplified CoW geometry. The patient-specific CoW geometry percentages of the flows in VA and ICA became 26% and 74%, respectively. Patient-specific CoW had a missing PCoA and different dimensions compared to the simplified case. Table 1 and fig. 2 show that when the peripheral resistances were reduced then the same trend in the VA and ICA flow rates movements was observed for the patient-specific case as for the simplified CoW geometry.

In fig. 3 the right ACA had a lower pressure due to the higher pressure drop in the remaining PCoA. The missing PCoA resulted in higher velocity in ACoA and ACA1 to deliver blood to the ACA2 (fig. 4). This result supports the predictions by Kim [20], which included an auto-regulation mechanism for a patient-specific CoW with a missing PCoA.

3.4 Current models and future model improvements

We used a number of different strategies in an effort to accurately simulate cerebral vascular flow. CFD can compute flow through patient-specific vascular geometries, but is a computationally intensive method that has limitations in terms of memory and processing speed. For the pipe network model the approach is to neglect much of the patient-specific spatial structure of the cerebral vascular system and to treat sections of the system as a network of pipes, where only the lengths and diameters of the pipes are derived from a particular patient. The advantage of using a pipe network is that for simple CoW geometries it may give nearly the same result as CFD, but with a much faster processing time.

The difference in VA and ICA flow rate predictions between the patient-specific and simplified CoW geometry highlighted the importance of using patient-specific geometry. In the future we plan to simulate further patient-specific geometries for the main CoW anatomical variations, to comprehensively investigate the effect of changes in the peripheral resistances of the CoW on the flow through the ICA and VA.

In our modelling we took into consideration the compliance of the blood vessel walls in the branching tree fractal model (which acts as an autoregulation mechanism), but did not include the active feedback control loop. Autoregulation

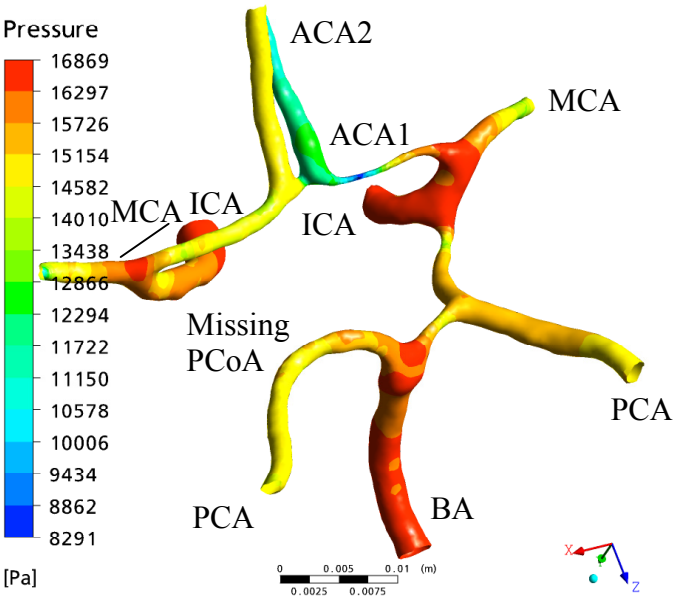

Figure 3: Instantaneous pressure distribution on the wall in the patient-specific CoW at peak systole. The two VA merge into the basilar artery (BA).

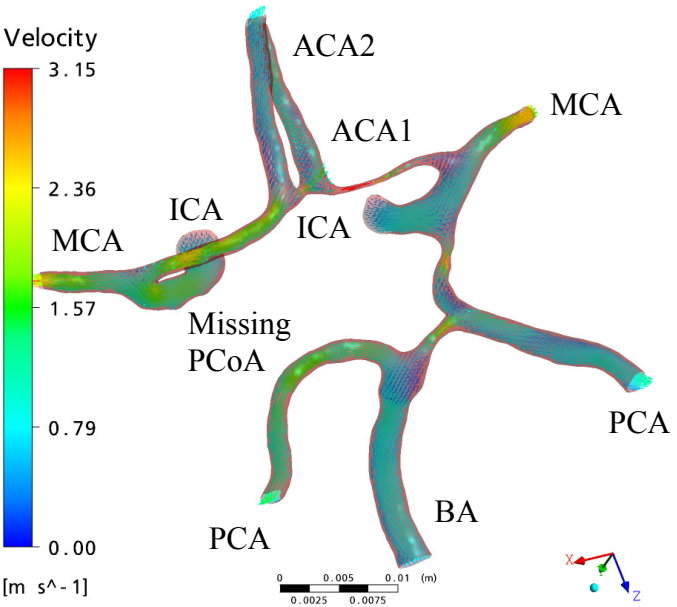

Figure 4: Instantaneous blood velocity in the patient-specific CoW at peak systole.

has been better modelled in previous CFD studies of CoW [14, 15, 17, 18, 19, 20] and we plan to incorporate such a method in our model.

Currently, our model has only one-way coupling between 3D CFD and the vascular tree fractal models. We are in the process of implementing a two-way coupling of the models that can more accurately predict the pressure variation within the CoW. The cerebral small vascular networks that often cannot be accurately obtained by medical imaging was modelled using a branching tree fractal model that accurately simulated the cerebral vasculature geometries and flow. This provided realistic pulsatile flow rate for the outlet arteries of the CoW. This fractal tree model also includes wall compliance and viscosity change due to artery size. Cebral *et al* [16] showed that blood simulated using a Newtonian model and a Casson non-Newtonian model in the CoW compared quite well, although the Newtonian model had lower wall shear stresses. In future we also plan to include non-Newtonian blood properties in the CFD model.

4 Conclusion

A coupled CFD model of the CoW and branching tree fractal model of the cerebral vasculature was used to investigate the effect of changes in the peripheral resistances of the CoW on the flow through the ICA and VA without occlusions. For the simplified CoW geometry the coupled model showed that a 10% decrease in diameters of the PCA peripheral vasculature predominately decreases the VA flow rate, while a 10% decrease in diameters of the ACA and MCA periphery vasculature predominately decreases the ICA flow rate.

A simple pipe network model predicted flows through the simplified CoW geometry were within 4% of the CFD predictions, but took much less time to compute. Thus, the simple network model can be useful tool to obtain general information about the flows in simple CoW geometries.

The coupled numerical model was also used to model the three-dimensional transient flow through a patient-specific CoW. It showed the same trends for changes in the peripheral resistances of the CoW on the flow through the ICA and VA, but the flow rate magnitudes differed due to the more complex geometry.

In future we will include:

- Two-way coupling between the 3D CFD and branching tree fractal models.
- An improved autoregulation model that includes an active feedback control loop.
- More patient-specific CoW geometries to simulate the main CoW anatomical variations when the CoW peripheral vascular resistances are changed.

References

[1] Kufahl, R.H. & Clark, M.E., A circle of Willis simulation using distensible vessels and pulsatile flow. *Journal of Biomechanical Engineering-Transactions of the ASME*, **107(2)**, pp. 112-122, 1985.

[2] Hillen, B., Hoogstraten, H.W. & Post, L. A mathematical model of the flow in the circle of Willis. *Journal of Biomechanics*, **19(3)**, pp. 187-194, 1986.
[3] Hillen, B., Drinkenburg, B.A.H., Hoogstraten, H.W. & Post, L., Analysis of flow and vascular-resistance in a model of the circle of Willis. *Journal of Biomechanics*, **21(10),** pp. 807-814, 1988.
[4] Cassot, F., Zagzoule, M. & Marc-Vergnes, J.P., Hemodynamic role of the circle of Willis in stenoses of internal carotid arteries. An analytical solution of a linear model. *Journal of Biomechanics*; **33(4)**, 395-405, 2000.
[5] Moorhead, K.T., Doran, C.V., Chase, J.G. & David, T., Lumped parameter and feedback control models of the auto-regulatory response in the circle of Willis, *Comput Methods Biome*, **7(3)**, pp. 121-130, 2004.
[6] Dickey, P.S., Kailasnath, P., Bloomgarden, G., Goodrich, I. & Chaloupka, J., Computer modeling of cerebral blood flow following internal carotid artery occlusion. *Neurological Research*, **18(3)**, pp. 259-266, 1996.
[7] Kailasnath, P., Dickey, P.S., Gahbauer, H., Nunes, J., Beckman, C. & Chaloupka, J.C., Intracarotid pressure measurements in the evaluation of a computer model of the cerebral circulation. *Surgical Neurology*, **50(3)**, pp. 257-263, 1998.
[8] Cieslicki, K. & Ciesla, D., Investigations of flow and pressure distributions in physical model of the circle of Willis. *Journal of Biomechanics*, **38(11)**, pp. 2302-2310. 2005.
[9] Roessler, F.C., Reith, W. & Siegel, G., Simulation of cerebral hemodynamics for preoperative risk assessment. *Brain Research*, **1118**, pp. 183-191, 2006.
[10] Alastruey, J., Parker, K.H., Peiro, J., Byrd, S.M. & Sherwin, S.J., Modelling the circle of Willis to assess the effects of anatomical variations and occlusions on cerebral flows. *Journal of Biomechanics,* **40(8)**, pp. 1794-1805, 2007.
[11] Matthys, K.S., Alastruey, J., Peiro, .J, Khir, A.W., Segers, P., Verdonck, P.R., Parker, K.H. & Sherwin, S.J., Pulse wave propagation in a model human arterial network: Assessment of 1-D numerical simulations against in vitro measurements. *Journal of Biomechanics*, **40(15)**, pp. 3476-3486, 2007.
[12] Ursino, M., Lodi, C.A. & Russo, G., Cerebral hemodynamic response to CO2 tests in patients with internal carotid artery occlusion: Modeling study and in vivo validation. *J Vasc Res*, **37(2)**, pp. 123-133, 2000.
[13] Viedma, A., Jimenez-Ortiz, C. & Marco, V., Extended Willis circle model to explain clinical observations in periorbital arterial flow. *Journal of Biomechanics,* **30(3),** 265-272, 1997.
[14] Fernandez, A., David, T. & Brown, M.D., Numerical models of auto-regulation and blood flow in the cerebral circulation. *Comp Meth Biomech En*, **5(1)**, pp. 7-19, 2002;
[15] David, T., Brown, M. & Ferrandez, A., Auto-regulation and blood flow in the cerebral circulation. *Int. J. Numer. Meth. Fluids*, **43**, 701-173, 2003.

[16] Cebral, J.R., Castro, M.A., Soto, O., Lohner, R. & Alperin, N., Blood-flow models of the circle of Willis from magnetic resonance data. *Journal of Engineering Mathematics,* **47(3-4)**, pp. 369-386, 2003.
[17] Moore, S., David, T., Chase, J.G., Arnold, J. & Fink, J., 3D models of blood flow in the cerebral vasculature. *Journal of Biomechanics*, **39(8)**, 1454-1463, 2006.
[18] Moore, S.M., Moorhead, K.T., Chase, J.G., David, T., & Fink, J., One-dimensional and three-dimensional models of cerebrovascular flow. *Journal of Biomechanical Engineering-Transactions of the ASME*, **127(3)**, pp. 440-449, 2005.
[19] Kim, C.S., Kiris, C., Kwak, D. & David, T., Numerical simulation of local blood flow in the carotid and cerebral arteries under altered gravity. *Journal of Biomechanical Engineering-Transactions of the ASME*, **128(2)**, pp. 194-202, 2006.
[20] Kim, C.S., Numerical simulation of auto-regulation and collateral circulation in the human brain. *Journal of Mechanical Science and Technology*, **21(3)**, pp. 525-535, 2007.
[21] Alnaes, M.S., Isaksen, J., Mardal, K.A., Romner, B., Morgan, M.K. & Ingebrigtsen, T., Computation of hemodynamics in the circle of Willis. *Stroke* **38(9)**, pp. 2500-2505, 2007.
[22] Bui, A., Šutalo, I.D., Manasseh, R. & Liffman, K, Dynamics of pulsatile flow in fractal models of vascular branching networks. *Med. & Biol. Eng. & Comp.* 2009.